Contents lists available at ScienceDirect

Process Safety and Environmental Protection

journal homepage: www.elsevier.com/locate/psep

Biomass valorization derivatives: Clean esterification of 2-furoic acid using tungstophosphoric acid/zirconia composites as recyclable catalyst

Angélica Escobar, Ángel Sathicq, Luis Pizzio, Mirta Blanco, Gustavo Romanelli**

Centro de Investigación y Desarrollo en Ciencias Aplicadas "Dr. Jorge J. Ronco" (CINDECA), Departamento de Química, Facultad de Ciencias Exactas, UNLP-CCT La Plata, CONICET, 47 N° 257, B1900AJK La Plata, Argentina

ARTICLE INFO

Article history:
Received 20 December 2014
Received in revised form 18 April 2015
Accepted 8 July 2015
Available online 17 July 2015

Keywords:
2-Furoic acid
Alkyl-2-furoates
Heteropolyacids/zirconia composites
Fragrances
Flavors
Biomass valorization

ABSTRACT

2-Furoic acid esters, which are biomass derived, are used in the flavoring and fragrance industry or as synthesis intermediates in the pharmaceutical industry. A series of zirconia samples modified with different contents of tungstophosphoric acid (TPA) and two different preparation methods ($ZrPEGTPA30_{T100}$, $ZrPEGTPA60_{T100}$, $ZrTPA30PEG_{T100}$, and $ZrTPA60PEG_{T100}$) were synthesized from zirconium propoxide via sol–gel reactions using polyethylene glycol as template. They were characterized by different physicochemical techniques (BET, FT-IR, ^{31}P MAS NMR and potentiometric titration), and their activities were tested in the synthesis of n-butyl-2-furoate as the model compound, among which $ZrTPA30PEG_{T100}$, (mesoporous acid zirconia modified catalyst) was the most active catalyst. The effect of various parameters such as catalyst loading, mole ratio of 2-furoic acid to n-butanol, and temperature was studied under optimized conditions. Several other alkyl 2-furoates were produced from esterification of 2-furoic acid with different alcohols using these catalysts, and the effect of alcohol structure over the conversion reaction was considered. The use of a solid acid catalyst made the procedure environmentally benign. The catalysts $ZrPEGTPA30_{T100}$ and $ZrTPA30PEG_{T100}$ were reused without appreciable loss of the catalytic activity (three runs). The methodology represents a green and efficient alternative for the conversion of bio-based 2-furoic acid into valuable esters.

1. Introduction

In the last two decades, the effective utilization of biomass for chemical and fuel production has emerged as a major research area (Lucas et al., 2014). Because the oil reserves could be exhausted, the development of novel, renewable, environmentally friendly chemicals and fuel sources is a growing need (Gallezot, 2007). Besides, and as reported by Serrano et al. (2012), this high reliance on fossil resources represents a serious issue in terms of environmental pollution, and the future development of society since these natural resources are highly contaminant. When looking into biomass constituents, it is possible to see their potential for making building block intermediates that can be transformed into a large number of families of useful or potentially useful products (Corma et al., 2007).

In this context, effective utilization of polysaccharides has attracted greater attention as a promising carbon-based

* *Corresponding authors*. Fax: +54 221 4211353.
E-mail addresses: lrpizzio@quimica.unlp.edu.ar (L. Pizzio), gpr@quimica.unlp.edu.ar (G. Romanelli).
http://dx.doi.org/10.1016/j.psep.2015.07.008
0957-5820/

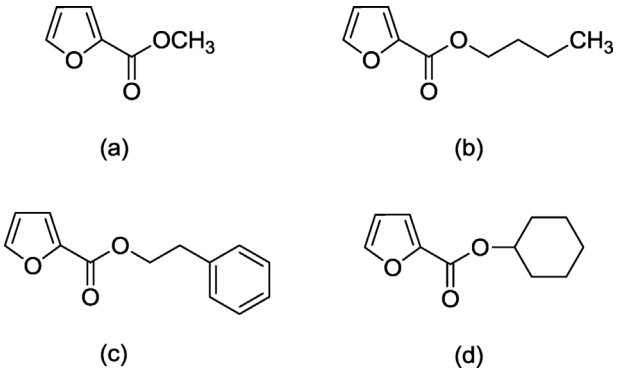

Fig. 1 – Furoate esters used as fragrance and flavoring agents. (a) Methyl-2-furoate, (b) n-butil-2-furoate, (c) 2-phenethyl-2-furoate, (d) cyclohexyl-2-furoate.

alternative source as it is a renewable and chemical feedstock (Corma et al., 2007; Lichtenthaler and Peters, 2004). The lignocellulosic biomass hydrolysis can lead to glucose, fructose and xylose, and subsequent dehydration of these monosaccharides generates 5-hydroxymetylfurfural and 2-furfural. These compounds are important building blocks widely applicable as coating agents, ecofriendly adhesives, biofuels and fine chemical products (Martínez et al., 2014; Lichtenthaler, 2000).

Furfural is an important renewable, nonpetroleum based, chemical feedstock. Hydrogenation of furfural provides furfuryl alcohol, which is a useful chemical intermediate that may be further hydrogenated to tetrahydrofurfuryl alcohol (THFA). THFA is used as a nonhazardous solvent in agricultural formulations and as an adjuvant to help herbicides penetrate the leaf structure. Furfural is used to make other chemicals derivatives, such as furoic acid, via oxidation, and furan via palladium catalyzed vapor phase decarbonylation (Corma et al., 2007; Lichtenthaler, 2000; Harrison and Moyle, 1956). The chemistry of furfural and its derivatives has been well and extensively reviewed by Zeitsch (2000) and Corma et al. (2007).

Furoic acid is used as a feedstock in organic syntheses and as an intermediate in the synthesis of medicines and perfumes. The same, it can be obtained from biomass particularly by furfural oxidation. In industrial use, 2-furoic acid is a preservative, acting as a bactericide and fungicide. It is also considered an acceptable flavoring ingredient characterized as a colorless liquid and has a distinct sweet, oily, herbaceous, and earthy odor. 2-Furoic acid is often used as a starting material for the production of furoate esters (Corma et al., 2007; Chamoulaud et al., 2001).

Particularly, esters are important derivatives that can be prepared using catalysts, including renewable feedstock based esters as fragrance and flavoring agents (Yadav and Yadav, 2014). Some relevant furoates, esters derivatives are shown in Fig. 1.

The preparation of furoate esters, which are an excellent renewable flavoring and fragrance agent, from 2-furoic acid using a heterogeneous acid catalyst under anhydrous condition is highly desirable. Traditional methods for the synthesis of 2-furoate esters include the Fischer esterification reaction for the condensation of the corresponding alcohols with 2-furoic acid using acid catalysts such as sulfuric acid (Klostergaard, 1958; Shaoyong et al., 2009), toluene-4-sulfonic acid (Polocci et al., 2013), thionyl chloride (Xu et al., 2013), chloro-trimethyl-silane (Mandal, 1983), potassium carbonate (Won et al., 2007a), chloridic acid (Zanetti and Beckmann, 1926), silica gel-immobilized perchloric acid (Chakraborti et al., 2009), among others. Other methods include: oxidative esterification of furfural using manganese (IV) oxide as catalyst (Chiarotto et al., 2013), reaction between 2-furoic acid with alkyl iodide using IRA 904 in acetonitrile as catalyst (Le Bigot et al., 1982), reaction between 2-furoylchloride and alcohols (D'Souza et al., 2006) and transesterification of methyl or ethyl 2-furoate using a long-chain alcohol catalyzed by 4 A molecular sieves (Martín-Muñoz et al., 1994).

Zirconium oxide (zirconia) is an interesting material to be used as catalyst support due to its thermal stability, and its basic and acid properties. The latter can be modified by the addition of cationic or anionic substances. For example, the addition of sulfate or tungstate ions has been widely studied, obtaining materials with high acidity (Yadav and Nair, 1999; Boyse and Ko, 1997).

The introduction of a heteropolyacid (HPA) in the zirconia matrix makes it an excellent catalyst with acidic properties. HPAs have several advantages, such as much flexibility in the modification of the acid strength, ease of handling, nontoxicity and environmental compatibility (Kozhevnikov, 1998). The preparation of HPA supported on zirconia employing the micellar method, with zirconyl chloride as oxide precursor, has been more extensively reported than the sol–gel method using a zirconium alkoxide. More recently, non-surfactant, low cost organic compounds, such as urea, have started to be used as pore-forming agents (Qu et al., 2007; Gords et al., 2010).

In the search of new technologies, with low environmental impact for the synthesis of organic compounds, our research group has reported some results about the use of TPA/zirconia, in the synthesis of quinoxalines (Sosa et al., 2013) and 14-aryl-14H-dibenzo [a, j] xanthenes (Rivera et al., 2012).

The present work demonstrates the efficient use of tungstophosphoric acid-modified mesoporous zirconia obtained from zirconium propoxide (precursor) and polyethylene glycol (pore-forming agent), as catalyst in the esterification of 2-furoic acid to 2-alkyl furoates. Various parameters for n-butyl-2-furoate synthesis were extensively investigated and validated against experimental results. The studies were extended to other esters.

2. Experimental

2.1. General

Chemicals were purchased from Aldrich, Fluka and Merck and were freshly used after purification by standard procedures (distillation and recrystallization). All the reactions were monitored by TLC on precoated silica gel plates (254 mm), GC and GC-MS analysis.

2.2. Catalyst preparation

A homogeneous solution of zirconium propoxide (Aldrich, 26.6 g) in absolute ethanol (Merck, 336.1 g) was prepared by stirring under nitrogen at room temperature. To catalyze the reaction by the sol-gel method, 0.47 cm^3 of 0.28 M HCl aqueous solution was added slowly to this mixture. It was allowed to stand for 3 h and then, a solution of polyethylene glycol (PEG)-alcohol-water (1:5:1 weight ratio) was added under vigorous stirring. Solutions were prepared in order to obtain tungstophosphoric acid (TPA) concentrations of 30 and 60% in the final solid. TPA were supported by two different methods, one was added together with PEG ($ZrPEGTPA30_{T100}$ and $ZrPEGTPA60_{T100}$ samples) and the other preparation,

TPA was added before PEG addition ($ZrTPA30PEG_{T100}$ and $ZrTPA60PEG_{T100}$ samples).

A sample without TPA addition was obtained with the aforementioned procedure ($ZrPEGTPA00_{T100}$).

The gels were then kept in a beaker at room temperature up to dryness, then were ground into powder and extracted with distilled water for three periods of 8 h, in a system with continuous stirring, to remove PEG. Afterwards, the solids were calcined at 100 °C for 24 h (indicated as sub index).

2.3. Catalyst characterization

The specific surface area and the mean pore diameter of the solids were determined from the N_2 adsorption–desorption isotherms at the liquid–nitrogen temperature, obtained using Micromeritics ASAP 2020 equipment. The solids were previously degassed at 100 °C for 2 h.

The ^{31}P magic angle spinning-nuclear magnetic resonance (^{31}P MAS NMR) spectra were recorded with Bruker Avance II equipment, using the CP/MAS ^{1}H–^{31}P technique. A sample holder of 4 mm diameter and 10 mm in height was employed, using 5 μs pulses, a repetition time of 4 s, and working at a frequency of 121.496 MHz for ^{31}P at room temperature. The spin rate was 8 kHz and several hundred pulse responses were collected. Phosphoric acid 85% was employed as external reference.

The Fourier transform infrared (FT-IR) spectra of the solids were obtained using Bruker IFS 66 FT-IR spectrometer and pellets in KBr in the 400–4000 cm^{-1} wavenumber range.

The acidity of the solids was estimated by means of potentiometric titration. A known mass of solid was suspended in acetonitrile and stirred for 3 h. Then, the suspension was titrated with 0.05 N n-butylamine in acetonitrile using Metrohm 794 Basic Titrino apparatus with a double junction electrode.

2.4. Catalytic test

A flask (25 cm^3 capacity) having a water reflux condenser was used as reactor. Predetermined amounts of reactants and the catalyst were charged into the flask and the temperature was raised to the set value. Once the temperature was attained, a zero hour sample was withdrawn and sampling was done periodically. The effect of different reaction temperatures, 2-furoic acid/n-butanol molar ratio and catalyst amounts were studied. The blank experiment conditions were: 1 mmol 2-furoic acid, 33 mmol n-butanol, temperature range 95–140 °C depending of the experiment, 24 h. The mixture was stirred at 700 rpm. Samples were withdrawn from the organic phase at different times (0.5, 1, 3, 5, 7, 9 and 24 h). Each sample volume was approximately 10 μL and was diluted with 100 μL of ethanol. The conversions were based on the limiting reactive determined by GC (Shimadzu, model 2014) using a FID detector and a capillary column (SPB-1, length 30 m, I.D. 32 mm, film thickness 1.00 μm) by calibration curve. The product was confirmed by GC-MS analysis (Perkin Elmer Auto System/Q-Mass 910). The Section 2 shows the mass spectra data of n-butyl-2-furoate.

2.5. General procedure for the alkyl-2-furoates

The catalyst was dried overnight prior to use. A mixture of 2-furoic acid (1 mmol), the corresponding alcohol (2 mmol) and the catalyst (50 mg) was placed in an open glass tube (20 mL) and stirred at 125 °C for 24 h. When the reaction time was over, the reaction mixture was extracted with acetone (3 cm^3), and the catalyst was filtered; the organic layer was dried over anhydrous sodium sulfate and the solvent evaporated. The crude product was purified by column chromatography on silica gel using a mixture of hexane-ethyl acetate (9:1) as eluent. Products were identified by comparison of the mass spectra of standard samples.

2.6. Catalyst reuse

Stability tests of the $ZrTPA30PEG_{T100}$ and $ZrPEGTPA30_{T100}$ catalysts were carried out running three consecutive experiments, under the same reaction conditions (2-furoic acid 1 mmol, n-butanol 2 mmol, the catalyst 50 mg, stirred at 125 °C for 24 h). After each test, the catalyst was separated from the reaction mixture by filtration, washed with toluene (2 × 2 cm^3), dried under vacuum, and then reused.

2.7. Quadrupole mass spectra of selected alkyl 2-furoates

n-Butyl-2-furoate (Pittelkow et al., 2004): *m/z* (*I* %): 168 (25) $M^{+\cdot}$, 112 (48), 95 (60), 84 (10), 68 (5), 56 (26), 53 (15), 44 (20), 39 (100), 32 (15), 28 (48).

Cyclohexyl-2-furoate (Lee et al., 2002): *m/z* (*I* %): 194 (5) $M^{+\cdot}$, 113 (30), 95 (27), 82 (10), 67 (20), 54 (41), 39 (100), 28 (55).

n-Hexyl-2-furoate (Won et al., 2007b): *m/z* (*I* %): 196 (19) $M^{+\cdot}$, 113 (57), 112 (44) 95 (45), 84 (4), 67 (4), 55 (32), 41 (77) 39 (100), 28 (62).

n-Octhyl-2-furoate (Tamura et al., 2012): *m/z* (*I* %): 224 (8) $M^{+\cdot}$, 113 (67), 112 (38), 95 (41), 55 (45), 44 (22), 43 (48), 41 (100), 39 (73) 28 (100).

n-Penthyl-2-furoate (Raja et al., 1989): *m/z* (*I* %): 182 (2) $M^{+\cdot}$, 113 (43), 112 (38), 95 (100), 70 (95), 55 (42), 43 (65), 39 (80).

3. Results and discussion

3.1. Catalyst characterization

The N_2 adsorption–desorption isotherms at the liquid–nitrogen temperature presented the main characteristics assigned to mesoporous materials and can be classified as type IV (see supplementary material).

The classification of common types of hysteresis published by Sing et al. (1985) provided a widely accepted correlation between the shape of hysteresis loops and the geometry and texture of the mesoporous adsorbent. Hysteresis is usually attributed to different size of pore mouth and pore body (this is the case of ink-bottle shaped pores) or to a different behavior in adsorption and desorption in near cylindrical through pores. However, according to Thommes et al. (2002) the shape and the width of sorption hysteresis loops depend both on the thermodynamic states of pore fluid and bulk fluid and pore diameter. Additionally, at temperatures below the bulk triple point they also depend strongly on the texture and degree of disorder) of the porous material.

In our samples, the hysteresis was hardly visible, which could be attributed to the presence of blind cylindrical or cone-shaped pores (Leofantia et al., 1998). On the other hand, the absence of the hysteresis for MCM-41 and titania modified with tungstophosphoric acid (Ajaikumar and Pandurangan, 2007; Fuchs et al., 2008a) was attributed to an ordered arrangement of the mesopores present in the material.

Table 1 – Textural properties of the solids calcined at 100 °C.

Sample	S_{BET} (m^2/g)	S_{Micro}[a] (m^2/g)	D_P[b] (nm)
$ZrPEGTPA00_{T100}$	396	6	2.8
$ZPEGTPA30_{T100}$	243	160	3.4
$ZPEGTPA60_{T100}$	213	140	3.6
$ZTPA30PEG_{T100}$	236	135	3.5
$ZTPA60PEG_{T100}$	198	106	3.2

[a] Micropore specific surface area estimated by the t-plot method.
[b] Mean pore diameter obtained from the specific BET surface area.

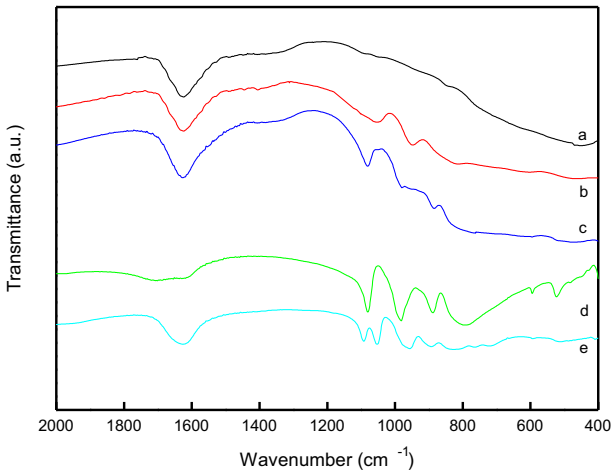

Fig. 2 – FT-IR spectra of $ZrPEGTPA00_{T100}$ (a), $ZrPEGTPA30_{T100}$ (b), and $ZrPEGTPA60_{T100}$ (c) samples; bulk TPA (d), and sodium salt of $[PW_{11}O_{39}]^{7-}$ anion (e).

The specific surface area (S_{BET}) of the samples determined from the N_2 adsorption–desorption isotherms using the Brunauer–Emmett–Teller (BET) method, the average pore diameter (D_P), and the micropore specific surface area (S_{Micro}) estimated from the t-plot method are listed in Table 1. The sample obtained without TPA addition ($ZrPEGTPA00_{T100}$) has the highest specific surface area. When TPA was added together with PEG, S_{BET} decreased and the microporosity (S_{Micro}) increased. When TPA was added before PEG ($ZrTPA30PEG_{T100}$ and $ZrTPA60PEG_{T100}$ samples), the decrease of both S_{BET} and S_{Micro} was slightly higher. The solids with higher TPA content ($ZrTPA60PEG_{T100}$ and $ZrTPAPEG60_{T100}$ samples) showed the lowest S_{BET}.

The S_{BET} decrease that takes place due to TPA addition can be attributed to a decrease in the cross-linking degree during the sol–gel synthesis when the acid concentration is increased. This is in agreement with reports in the literature that indicate a similar behavior for the specific surface of mesoporous titania obtained via the sol–gel process (Fuchs et al., 2008a; Phonthammachai et al., 2003; Khalil et al., 1998).

The FT-IR spectrum of the $ZrPEGTPA00_{T100}$ sample (Fig. 2) showed an intense band between 3600 and 3200 cm^{-1} and another one at 1600 cm^{-1}, assigned to the stretching vibrations of hydroxo- and aquo-OH, and to the bending vibration of (H—O—H) and (O—H—O) present in the structure of the solid, respectively (Patel et al., 2003; Rubio et al., 1997; Rob Van Veen et al., 1985). Additionally, the wide band due to Zr–O stretching vibration was observed in the energy interval below 850 cm^{-1}.

The FT-IR spectra of the $ZrPEGTPA30_{T100}$ and $ZrPEGTPA60_{T100}$ samples displayed a new set of bands overlapped to the zirconia wide band. The presence of the P—O_a (1081 cm^{-1}), W—O_d (982 cm^{-1}), and W—O_b—W (888 cm^{-1}),

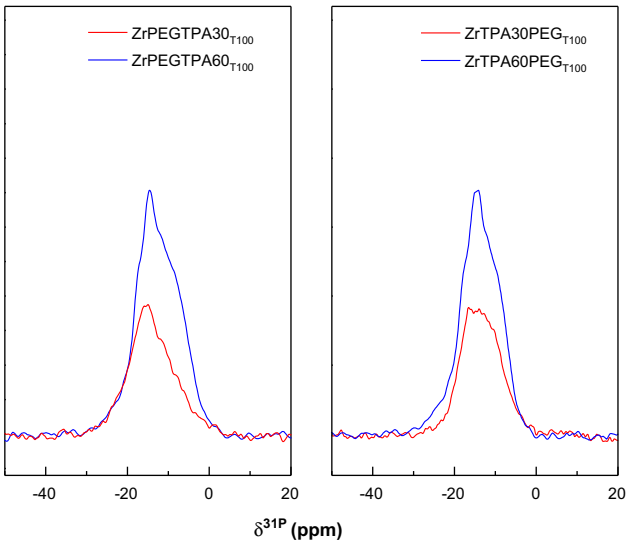

Fig. 3 – ^{31}P MAS NMR spectra of $ZrPEGTPA30_{T100}$, $ZrPEGTPA60_{T100}$, $ZrTPA30PEG_{T100}$, and $ZrTPA60PEG_{T100}$ samples.

stretching vibrations characteristic of the $[PW_{12}O_{40}]^{3-}$ anion (Rob Van Veen et al., 1985) can be clearly observed in the case of the $ZrPEGTPA60_{T100}$ sample. In addition, bands assigned to the $[PW_{11}O_{39}]^{7-}$ anion are also observed in the case of the $ZrPEGTPA60_{T100}$ sample if a comparison with the spectrum of the sodium salt of the lacunary anion is made, which presents bands at 1100, 1046, 958, 904, 812, and 742 cm^{-1} (Fig. 2), in agreement with the literature (Rocchiccioli-Deltcheff et al., 1976). The FT-IR spectra of $ZrTPA30PEG_{T100}$ and $ZrTPA60PEG_{T100}$ samples displayed the same main features as those of $ZrPEGTPA30_{T100}$, and $ZrPEGTPA60_{T100}$ samples, respectively. So, according to FT-IR results, the order employed for PEG incorporation during the synthesis did not generate significant differences in the polyoxotungstates species present in the solid.

Additionally, the FT-IR spectra of the samples after being leached with distilled water did not present any of the characteristic bands of PEG, such as that assigned to the C—O stretching mode of the ether group of PEG at 1099 cm^{-1} (Jung et al., 2004), showing that the template removal by water extraction was effective.

Fig. 3 shows the ^{31}P MAS NMR spectra of $ZrPEGTPA30_{T100}$, $ZrPEGTPA60_{T100}$, $ZrTPA30PEG_{T100}$, and $ZrTPA60PEG_{T100}$ samples. The ^{31}P MAS NMR spectrum of the $ZrPEGTPA60_{T100}$ sample displayed a wide band with a maximum at around −14 ppm, accompanied by a shoulder at −12 ppm. They were attributed to the $[PW_{12}O_{40}]^{3-}$ anion and to the $[P_2W_{21}O_{71}]^{6-}$ dimeric species, respectively (Massart et al., 1977). The downfield shift and the increase of the line width observed, compared to the TPA (−15.3 ppm), can be ascribed to the interaction between the anion and the zirconia matrix (Mastikhin et al., 1990; López-Salinas et al., 2000). The interaction can be assumed to be of the electrostatic type due to the transfer of protons to Zr–OH (Jung et al., 2004) according to: $Zr–OH + H_3PW_{12}O_{40} \rightarrow [Zr–OH_2^+]_n[H_{3-n}PW_{12}O_{40}]^{n-}$.

The same wide band with a shoulder assigned to $[PW_{12}O_{40}]^{3-}$ and $[P_2W_{21}O_{71}]^{6-}$ respectively, was also present in the ^{31}P MAS NMR spectrum of $ZrPEGTPA30_{T100}$ sample.

On the other hand, ^{31}P MAS NMR spectra of $ZrTPA30PEG_{T100}$, and $ZrTPA60PEG_{T100}$ samples showed the same features as those of $ZrPEGTPA30_{T100}$, and

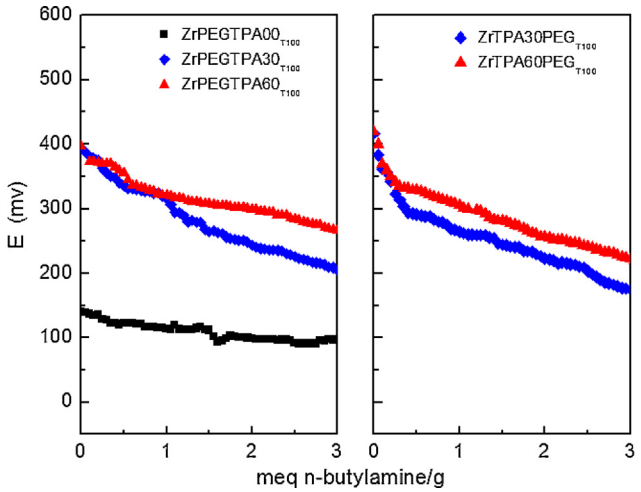

Fig. 4 – Potentiometric titration curves of $ZrPEGTPA00_{T100}$, $ZrPEGTPA30_{T100}$, $ZrPEGTPA60_{T100}$, $ZrTPA30PEG_{T100}$, and $ZrTPA60PEG_{T100}$ samples.

$ZrPEGTPA60_{T100}$ samples. However, for the $ZrTPA30PEG_{T100}$ sample, the intensity of the shoulder assigned to $[P_2W_{21}O_{71}]^{6-}$ dimeric species is higher than in the case of $ZrPEGTPA30_{T100}$.

Taking into account the FT-IR and ^{31}P MAS NMR results, it can be established that the $[PW_{12}O_{40}]^{3-}$ anion is the main species in the samples. However, it was partially transformed into $[P_2W_{21}O_{71}]^{6-}$ and $[PW_{11}O_{39}]^{7-}$ anions during the synthesis and drying steps. According to Pope (1983), the transformation is due to the limited stability range of the $[PW_{12}O_{40}]^{3-}$ anion in solution. He suggested that the following transformation scheme: $[PW_{12}O_{40}]^{3-} \Leftrightarrow [P_2W_{21}O_{71}]^{6-} \Leftrightarrow [PW_{11}O_{39}]^{7-}$ occurred when the hydroxyl concentration was increased. This may be considered as a valid path followed by the TPA species during the synthesis of the samples.

The acidity measurements of the catalysts by means of potentiometric titration with n-butylamine let us estimate the number of acid sites and their acid strength. It was suggested that the initial electrode potential (E_i) indicates the maximum acid strength of the sites and the area under the E_i versus meq amine/g solid curve represents the total number of acid sites per gram of catalyst (N_{GC}). The acid strength of these sites may be classified considering to the following scale: $E_i > 100$ mV (very strong sites), $0 < E_i < 100$ mV (strong sites), $-100 < E_i < 0$ (weak sites), and $E_i < -100$ mV (very weak sites) (Cid and Pecci, 1985; Fuchs et al., 2008b).

According to the above-mentioned scale, the unmodified sample $ZrPEGTPA00_{T100}$ ($E_i = 140$ mV) displayed very strong acid sites. On the other hand, the acid strength of the modified samples $ZrPEGTPA30_{T100}$ ($E_i = 394$ mV), $ZrPEGTPA60_{T100}$ ($E_i = 397$ mV), $ZrTPA30PEG_{T100}$ ($E_i = 416$ mV), and $ZrTPA60PEG_{T100}$ ($E_i = 420$ mV) markedly increased (Fig. 4) though it is lower than that of bulk TPA ($E_i = 620$ mV) (Pizzio and Blanco, 2003).

The acid strength of the solids obtained adding the TPA before PEG ($ZrTPA30PEG_{T100}$, and $ZrTPA60PEG_{T100}$ samples) was slightly higher than that of the ones prepared adding them simultaneously ($ZrPEGTPA30_{T100}$ and $ZrPEGTPA60_{T100}$ samples). However, the acid strength was almost independent of the TPA concentration. The lower acid strength of the tungstophosphoric acid/zirconia composites compared to bulk TPA could be due to the fact that the protons in $H_3PW_{12}O_{40}\cdot 6H_2O$ are present as $H^+(H_2O)_2$ species, whereas in the $ZrTPA60PEG_{T100}$ and $ZrPEGTPA30_{T100}$ samples, they are interacting with the oxygen of Zr-OH groups or in a higher hydration state ($H^+(H_2O)_n$). This is in agreement with previous work (Pizzio and Blanco, 2003) reporting that $H_3PW_{12}O_{40}\cdot 21H_2O$, where the protons are highly hydrated, displayed lower acid strength ($E_i = 538$ mV) than $H_3PW_{12}O_{40}\cdot 6H_2O$, while the partially substituted salts $Cs(K)_{2.9}H_{0.1}PW_{12}O_{40}$ containing bare protons showed E_i in the range 900–1000 mV.

On the other hand, the number of acid sites N_{GC} of $ZrTPA60PEG_{T100}$ and $ZrPEGTPA60_{T100}$ samples was similar. The same behavior was found in the case of $ZrTPA30PEG_{T100}$ and $ZrPEGTPA30_{T100}$ catalysts. Therefore, N_{GC} values did not depend on the time elapsed between the template PEG solution addition and TPA incorporation. Additionally, N_{GC} values (expressed per gram of catalyst) of $ZrTPA60PEG_{T100}$ and $ZrPEGTPA60_{T100}$ samples were slightly higher than those of $ZrTPA30PEG_{T100}$ and $ZrPEGTPA30_{T100}$. However, if the number of acid sites was expressed per gram of TPA (N_{GTPA}), the samples $ZrTPA30PEG_{T100}$ and $ZrPEGTPA30_{T100}$ displayed values significantly higher than those of the $ZrTPA60PEG_{T100}$ and $ZrPEGTPA60_{T100}$ solids. According to these results, the increment of the TPA content from 30% to 60% did not lead to significantly increase the number of acid sites in the catalyst.

3.2. *Catalytic tests*

The reaction of 2-furoic acid with n-butanol in the presence of $ZrTPA30PEG_{T100}$, $ZrPEGTPA60_{T100}$, $ZrPEGTPA30_{T100}$ and ZrTPA60PEGT100 catalysts was chosen as model reaction for Fischer esterification studies (Scheme 1).

The esterification was carried out at 140 °C using 1 mmol of 2-furoic acid, 33 mmol of n-butanol and the tungstophosphoric acid/zirconia composites synthesized. The amount of catalyst employed was 200 mg in the case of $ZrTPA30PEG_{T100}$ and $ZrPEGTPA30_{T100}$ samples, and 100 mg for $ZrPEGTPA60_{T100}$ and $ZrTPA60PEG_{T100}$, in order to keep TPA amount constant. It is important to be remarked that the n-butyl-2-furoate is the unique detected product in all the reaction carried out in the work, indicating that the yield to this product is equal to the attained conversion (n-buthyl-2-furoate selectivity 100%). Additionally, the procedure was performed in solvent-free condition, representing a clean and friendly alternative to the environment.

The reaction profiles are shown in Fig. 5, and the conversion of 2-furoic acid after 24 h of the reaction are listed in Table 2.

The esterification of 2-furoic acid with alcohols proceeds even in the absence of catalyst, because 2-furoic acid itself shows acidity capable of catalyzing the reaction. For example, Kuwahara et al. (2014) showed that in the absence of catalyst levulinic acid can be esterified with ethanol at 70 °C (1.8% in 10 h). Before attempting detailed catalytic work, a noncatalytic reaction using 2-furoic acid, and n-butanol was examined and it was observed that, under the same above mentioned experimental conditions, only a conversion of 10% was detected

Table 2 – Acidity properties and reaction conversion (%).

Entry	Catalyst	E_i (mV)	Conversion (%)[a]
1	None		10
2	$ZPEGTPA30_{T100}$	394	90
3	$ZPEGTPA60_{T100}$	397	79
4	$ZTPA30PEG_{T100}$	416	95
5	$ZTPA60PEG_{T100}$	420	75

[a] Conversion % determined by CG analysis at 24 h an 140 °C.

Scheme 1 – Model esterification reaction between 2-furoic acid and n-butanol.

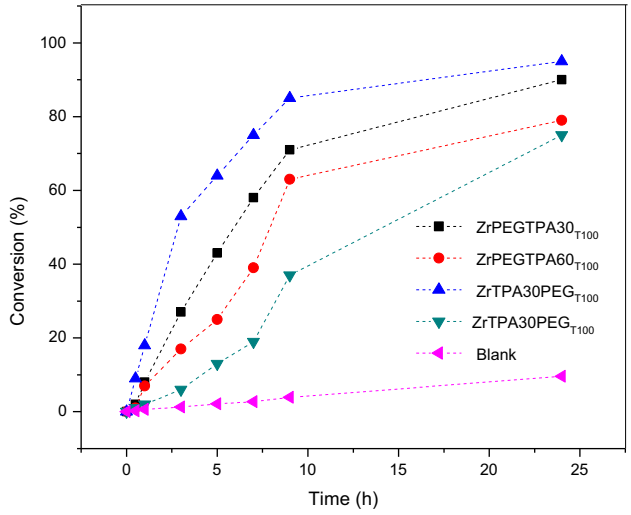

Fig. 5 – Conversion of 2-furoic acid as a function of time for the different synthesized catalysts. Reaction conditions: 2-furoic acid, 1 mmol; n-butanol, 33 mmol; 100 mg of ZrPEGTPA60$_{T100}$ and ZrTPA60PEG$_{T100}$ catalysts or 200 mg of ZrPEGTPA30$_{T100}$ and ZrTPA30PEG$_{T100}$ catalysts; 60% active phase, temperature 140 °C, stirring.

at 24 h (Fig. 5), indicating that from a practical point of view the reaction is not taking place in an important extent in the absence of a catalyst.

As shown in Fig. 5, the reaction was significantly accelerated in the presence of the solid acid catalysts. It can be observed that the conversion, increased faster when ZrTPA30PEG$_{T100}$ and ZrPEGTPA30$_{T100}$ solid were employed compared to those prepared with 60% TPA concentration. Additionally, taking into account that the conversion obtained at 24 h under reaction with ZrTPA30PEG$_{T100}$ and ZrPEGTPA30$_{T100}$ catalysts changed litter (95% and 90%, respectively, as shown in Table 2), the catalytic activity seems to be slightly independent of the time elapsed between the template PEG solution addition and TPA incorporation. A similar behavior was observed for the ZrTPA60PEG$_{T100}$ and the ZrPEGTPA60$_{T100}$ catalysts (75% an 79%, respectively, see Table 2).

Considering that the maximum acid strength of the ZrTPA30PEG$_{T100}$ and ZrPEGTPA30$_{T100}$ samples (E_i = 394 and 416 mV, respectively) was almost similar to those of the ZrTPA60PEG$_{T100}$ and ZrPEGTPA60$_{T100}$ solid (E_i = 397 and 420 mV, respectively), the higher yield obtained using the ZrTPA30PEG$_{T100}$ and ZrPEGTPA30$_{T100}$ samples can be attributed, to the fact that these materials displayed a higher number of acid sites per gram of TPA (N_{GTPA}) than ZrTPA60PEG$_{T100}$ and ZrPEGTPA60$_{T100}$ solid (Fig. 4).

Here, it is important to be remarked that the n-butyl-2-furoate is the unique detected product in all the reaction carried out in the work, thus indicating that the yield to this product is equal to the attained conversion.

Then, the influence of the temperature on n-butyl-2-furoate synthesis was investigated using the ZrTPA30PEG$_{T100}$ and ZrPEGTPA30$_{T100}$ catalysts, and the results are illustrated in Fig. 6a and b. In order to estimate the optimal temperature,

Table 3 – Effect of the 2-furoic acid/n-butanol molar ratio.

Entry	Molar ratio acid:alcohol	Conversion (%)[a]
1	1:2	82
2	1:6	63
3	1:11	36
4	1:33	18

Reaction conditions: 2-furoic acid, 1 mmol; ZrTPA30PEG$_{T100}$ catalyst, 50 mg; reaction time 10 h; 125 °C; stirring.

[a] Conversion % determined by GC analysis.

five temperatures (70, 95, 110, 125 and 140 °C) were tested. No reaction was observed at 70 °C. A temperature increase leads to a higher 2-furoic acid conversion. For example, for a reaction time of 24 h at 110 °C, it was only 25%, using the ZrTPA30PEG$_{T100}$ catalyst whereas, at 125 °C the conversion was 93% (see Fig. 6a). Similarly, the yield to n-butyl-2-furoate using the ZrPEGTPA30$_{T100}$ catalyst, for a reaction time of 24 h at 110 °C was only 22%, whereas at 125 °C the conversion was 80%, and at 140 °C the conversion was 90% (Fig. 6b).

Fig. 7a and b displays the effect of the amount of ZrTPA30PEG$_{T100}$ or ZrPEGTPA30$_{T100}$ catalysts, respectively, on the yield to n-butyl-2-furoate in the studied esterification reaction. A variable amount of these catalysts (50, 100, 150 and 200 mg) was used. It can be seen that the conversion increased from 65% to 90% when the amount of ZrTPA30PEG$_{T100}$ increased from 50 to 100 mg (Fig. 7a). No relevant change of conversion was observed with further increase in the amount of ZrTPA30PEG$_{T100}$ reaching only 95% when using 200 mg of catalyst (Fig. 7a). Thus 100 mg is the suitable amount in this reaction. A quite similar result was obtained when using the ZrPEGTPA30$_{T100}$ catalyst (Fig. 7b).

Table 3 displays the effect of the 2-furoic acid/n-butanol molar ratio on the attained conversion of 2-furoic acid. A variable amount of n-butanol was employed (2, 6, 11 and 33 mmol respectively). It can be observed that only a 2-furoic acid/n-butanol molar ratio 1:2 is sufficient to improve the ester yield (Table 3), obtaining a 2-furoic acid conversion of 82% at 10 h under reaction. This result represents an excellent outcome in terms of reduction of the E factor (Sheldon, 2000); for this reason these conditions were used in the next experiments.

In the present work, we explore a reaction where one of the reagents also acts as reaction solvent. The conversion of substrate as a function of n-butanol amount showed that an increase in n-butanol reduces the conversion of 2-furoic acid. It is well known that a reduction in solvent leads to a solvent-free process, and the reaction rate increases notably. In this condition, the reaction rate is at its maximum because in the rate constant the concentration of reactants reaches its maximum as well. It is also logical to say that the reagents and the catalyst are in close proximity. Finally, another possible effect that may reduce the reaction rate can be a solvation effect of n-butanol on one of the reagents (2-furoic acid), which prevents its approach to the catalyst.

The reusability of the ZrTPA30PEG$_{T100}$ and ZrPEGTPA30$_{T100}$ catalysts was investigated in the sequential reaction of esterification between 2-furoic acid and n-butanol. At the end of each run the catalyst was removed by filtration, washed with

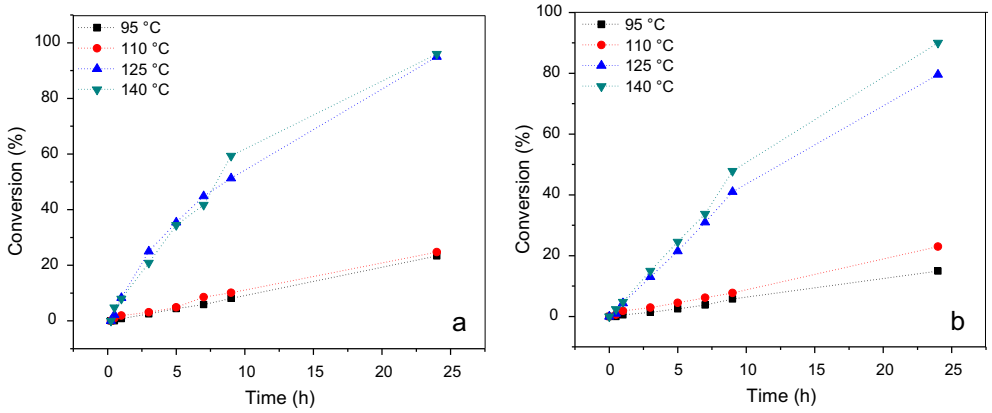

Fig. 6 – Conversion (%) of 2-furoic acid to n-butyl-2-furoate as a function of time (h). Effect of reaction temperature. (a) ZrTPA30PEG$_{T100}$ catalyst, (b) ZrPEGTPA30$_{T100}$ catalyst. Reaction conditions: 2-furoic acid, 1 mmol; n-butanol, 33 mmol; catalyst 200 mg (60% active phase); stirring.

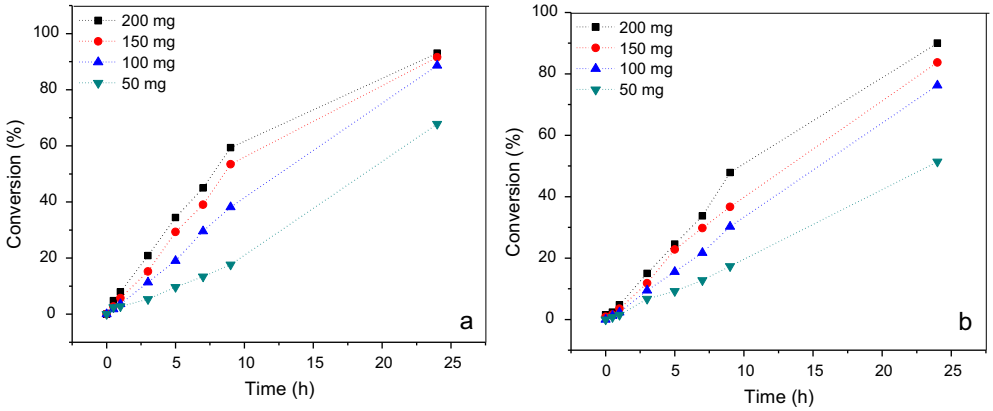

Fig. 7 – Conversion (%) of 2-furoic acid to n-butyl-2-furoate as a function of time. Effect of the amount of catalyst. (a) ZrTPA30PEG$_{T100}$, (b) ZrPEGTPA30$_{T100}$. Reaction conditions: 2-furoic acid, 1 mmol; n-butanol, 33 mmol, 125 °C; stirring.

n-butanol, dried in vacuum at 40 °C and reused. The results showed that both catalysts can be reused in three consecutive runs with no appreciable loss of their catalytic activity (the yield was 95% in all three cases).

In order to evaluate the possible catalyst solubilization, an additional test was performed. The ZrTPA30PEG$_{T100}$ catalyst was refluxed in 3 cm^3 of n-butanol for 24 h, filtered and dried in vacuum till constant weight. The refluxed n-butanol was used as solvent for attempting the reaction without adding the catalyst. After 10 h, the yield of n-butyl-2-furoate was only 6%, compared to 51% obtained with the ZrTPA30PEG$_{T100}$ catalyst or 4% in the blank experiment.

To explore the potential of this catalytic system and extend the scope of this method, the esterification of 2-furoic acid with various alcohols (primary, secondary, tertiary and benzylic), was studied. The reactivity of the selected compounds was tested using the same reaction conditions (2-furoic acid 1 mmol, the corresponding alcohol 2 mmol and the catalyst 50 mg and stirred at 125 °C for 24 h) and alternatively ZrTPA30PEG$_{T100}$, and ZrPEGTPA30$_{T100}$ as catalysts, which are the solids that gave the highest yields of n-butyl-2-furoate. The results of the obtained yields are listed in Table 4. It must be pointed out that the reactions were clean and the products were isolated by liquid column chromatography in pure form without further purification. The reactions were very selective and in general no competitive side reactions took place, as the gas-chromatography/mass spectrometry analysis showed.

However, an important effect of the alcohol structure on the yield to the reaction products was found. The steric component affecting alcohol reactivity is also a decisive factor for Fischer acid-catalyzed esterification (Osiglio et al., 2010). Steric hindrance increases with molecular size, inducing electronic repulsion between nonbonded atoms of the reacting molecules. This repulsive hindrance decreases the electronic density in the intermolecular region and disturbs the bonding interaction (Liu et al., 2006).

The reactivity of primary and benzylic alcohols (Table 4, entries 3–7, 11 and 12) was higher than that of the secondary alcohols (Table 4, entries 9, 14–16). The yield difference between primary and secondary alcohols can be attributed to steric effects that considerably affect the esterification. The presence of bulky groups, for example diphenylcarbinol (Table 4, entry 15) not far from the reaction center, either in the alcohol or in the acid, slows down the esterification rate, in our case, where the most sterically hindered alcohols give a lower yield. Similarly, very bulky menthol (a secondary alcohol) and triphenylmethanol (a tertiary alcohol) give only traces or no reaction is detected under similar reaction condition (Table 4, entries 13 and 16). In sum, the reactivity order toward esterification of 2-furoic acid with alcohols was as follows: primary alcohols > secondary alcohols > tertiary alcohol.

Finally, methanol and ethanol were tested at the reflux temperature of 69 and 78 °C respectively. In these conditions, no conversion of substrates was obtained indicating that a high temperature is necessary for the reaction to take place.

Table 4 – Effect of various alcohol substrates on the esterification of 2-furoic acid.

Entry	Reactive	Catalyst	Product	Conversion (%)
1[a]	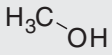	$ZrTPA30PEG_{T100}$	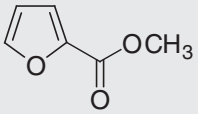	–
2[b]	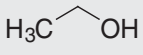	$ZrTPA30PEG_{T100}$	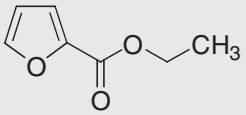	–
3	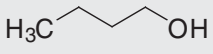	$ZrTPA30PEG_{T100}$	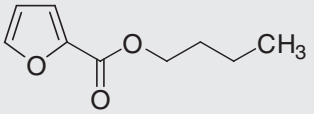	97
4	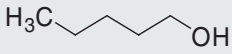	$ZrTPA30PEG_{T100}ZrPEGTPA30_{T100}$	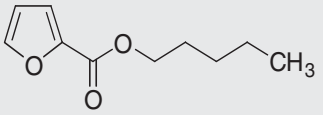	9590
5	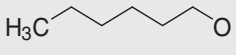	$ZrTPA30PEG_{T100}$	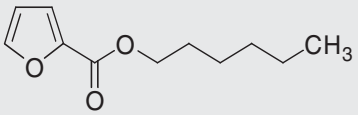	89
6	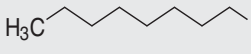	$ZrTPA30PEG_{T100}ZrPEGTPA30_{T100}$	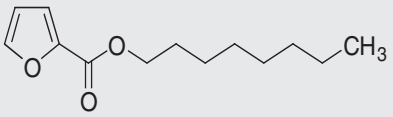	9998
7	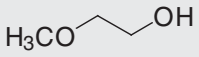	$ZrTPA60PEG_{T100}$	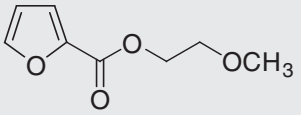	65
8	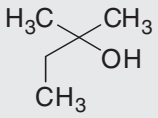	$ZrPEGTPA30_{T100}$	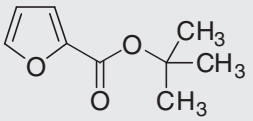	25
9	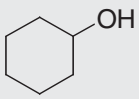	$ZrTPA30PEG_{T100}$	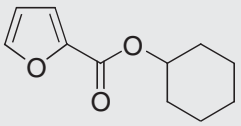	60
10	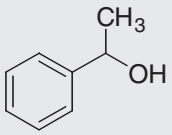	$ZrTPA30PEG_{T100}$	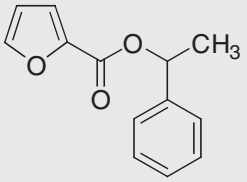	Traces
11	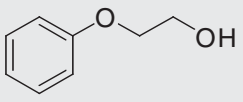	$ZrTPA30PEG_{T100}ZrPEGTPA30_{T100}$	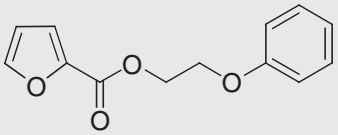	8380
12	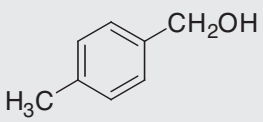	$ZrTPA30PEG_{T100}$	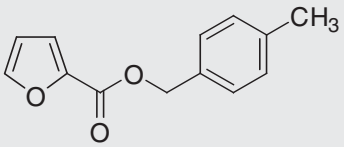	79

– Table 4 (*Continued*)

Entry	Reactive	Catalyst	Product	Conversion (%)
13	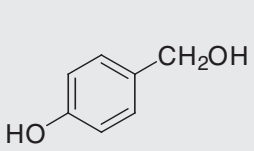	$ZrTPA30PEG_{T100}$	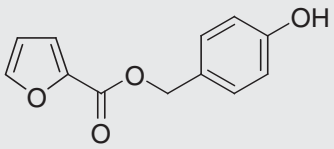	–
14	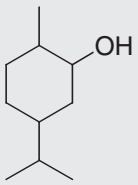	$ZrTPA30PEG_{T100}$	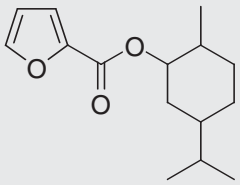	Traces
15	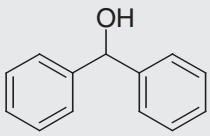	$ZrTPA30PEG_{T100}$	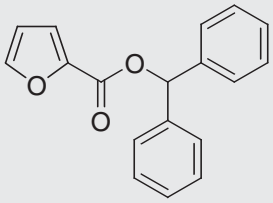	Traces
16	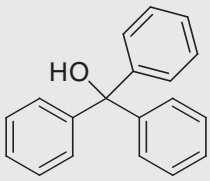	$ZrTPA30PEG_{T100}$	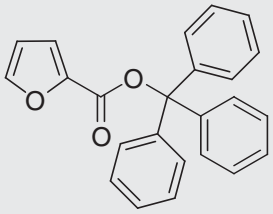	–

Reaction conditions: 2-furoic acid, 1 mmol; alcohol, 2 mmol; solvent-free; catalyst 50 mg reaction time 24 h; 125 °C; stirring.

[a] The reaction was performed at 65 °C.

[b] The reaction was performed at 78 °C.

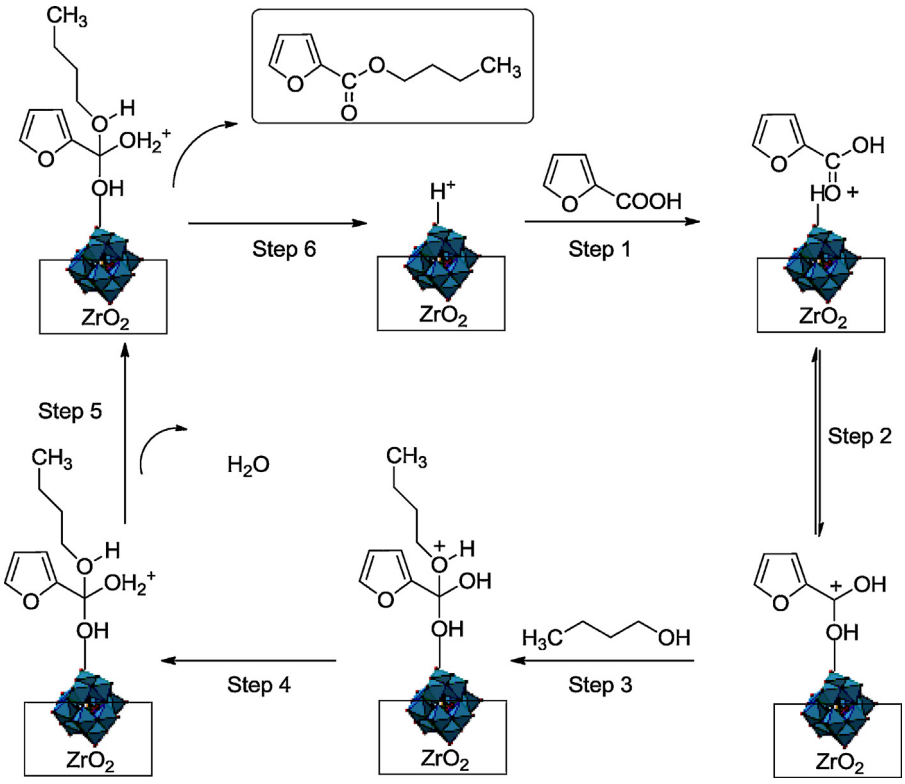

Scheme 2 – .

Due to the characteristics of the catalysts prepared here, they may present Brønsted sites (Madje et al., 2004), so we assume that the type of sites affects the esterification activity. The mechanism of the reaction can be described as proceeding through the adsorption of 2-furoic acid on Brønsted sites, forming a protonated 2-furoic acid intermediate, as shown in Scheme 2. The alcohol would react with this protonated intermediate to form the corresponding ester and water. The different step of the procedure are listed below:

The reaction mechanism for the esterification of 2-furoic acid with alcohols could be described as a general Fischer esterification and has several steps: 1 – adsorption of 2-furoic acid on the catalyst surface, forming a protonated 2-furoic acid intermediate, and increases the electrophilicity of carbonyl carbon; 2 – the carbonyl carbon is attacked by the nucleophilic oxygen atom of the alcohol leading to the formation of an oxonium ion; 3 – a proton transfer in the oxonium ion gives a new oxonium ion; 4 – the loss of water from the latter oxonium ion; 5 – deprotonation leads to the ester, being regenerated the acid site on the catalyst surface.

4. Conclusion

Esters of 2-furoic acid are used as flavoring and fragrance agents, and as intermediates in the pharmaceutical industry. In this paper, a variety of tungstophosphoric acid/zirconia composite materials were prepared using PEG as pore-forming agent, via sol–gel reactions, and were employed for the synthesis of alkyl 2-furoates using 2-furoic acid and various alcohols. The model reaction was Fischer esterification of 2-furoic acid with n-butanol. It was found that the catalyst behavior in this reaction may be related to the number of acid sites that the materials present. The $ZrTPA30PEG_{T100}$ material, a mesoporous solid with high strength and number of acid sites, was the best catalyst for the studied esterification. The catalyst was found active, stable, and reusable for the esterification reaction of not only n-butanol but also a wide range of alcohols. The alcohol structure is a key in the conversion to the esterification product. The reactivity order toward esterification with 2 furoic acid using tungstophosphoric acid/zirconia composite materials was as follows: primary alcohols > secondary alcohols > tertiary alcohol, and depended strongly on a steric effect of the alcohol structure. The effect of various parameters such as catalyst loading, 2-furoic acid to n-butanol molar ratio, and reaction temperature was studied. Additionally, a solvent-free condition, excellent reaction yields, a straightforward procedure, and relative nontoxicity of the catalyst are other noteworthy advantages of this method. Finally, these solid acid catalysts can be recovered and reused at least three times with negligible loss in their activity.

Acknowledgements

The authors thank ANPCyT, CONICET and Universidad Nacional de La Plata, for financial support, and M. Baez, L. Soto, and L. Osiglio, for their collaboration in the experimental measurements.

Appendix A. Supplementary data

Supplementary data associated with this article can be found, in the online version, at http://dx.doi.org/10.1016/j.psep.2015.07.008.

References

Ajaikumar, S., Pandurangan, A., 2007. Esterification of alkyl acids with alkanols over MCM-41 molecular sieves: influence of hydrophobic surface on condensation reaction. J. Mol. Catal. A: Chem. 266, 1–10.

Boyse, R., Ko, E., 1997. Crystallization behavior of tungstate on zirconia and its relationship to acidic properties. 1. Effect of preparation parameters. J. Catal. 171, 191–207.

Chakraborti, A., Singh, B., Chankeshwara, S., Patel, A.R., 2009. Protic acid immobilized on solid support as an extremely efficient recyclable catalyst system for a direct and atom economical esterification of carboxylic acids with alcohols. J. Org. Chem. 74, 5967–5974.

Chamoulaud, G., Floner, D., Moinet, C., Lamy, C., Belgsir, E.M., 2001. Biomass conversion II: simultaneous electrosyntheses of furoic acid and furfuryl alcohol on modified graphite felt electrodes. Electrochim. Acta 46, 2757–2760.

Chiarotto, I., Feroci, M., Sotgiu, G., Inesi, A., 2013. The dual role of ionic liquid BmimBF4, precursor of N-heterocyclic carbene and solvent, in the oxidative esterification of aldehydes. Tetrahedron 69 (37), 8088–8095.

Cid, R., Pecci, G., 1985. Potentiometric method for determining the number and relative strength of acid sites in colored catalysts. Appl. Catal. A: Gen. 14, 15–21.

Corma, A., Iborra, S., Velty, A., 2007. Chemical routes for the transformation of biomass into chemicals. Chem. Rev. 107, 2411–2502.

D'Souza, M.J., Boggs, M.E., Kellin, D.N., 2006. Correlation of the rates of solvolysis of 2-furancarbonyl chloride and three naphthoyl chlorides. J. Phys. Org. Chem. 19, 173–178.

Fuchs, V.M., Soto, E.L., Blanco, M.N., Pizzio, L.R., 2008a. Direct modification with tungstophosphoric acid of mesoporous titania synthesized by urea-templated sol–gel reaction. J. Colloid Interface Sci. 327, 403–411.

Fuchs, V.M., Pizzio, L.R., Blanco, M.N., 2008b. Synthesis and characterization of aluminum or copper tungstophosphate and tungstosilicate immobilized in a polymeric blend. Eur. Polym. J. 44, 801–807.

Gallezot, P., 2007. Process options for converting renewable feedstocks to bioproducts. Green Chem. 9, 295–302.

Gords, M.N., Blanco, M.N., Pizzio, L.R., 2010. Synthesis and characterization of catalysts obtained by trifluoromethanesulfonic acid immobilization on zirconia. Stud. Surf. Sci. Catal. 175, 405–408.

Harrison, R.J., Moyle, M., 1956. Org. Synth. 36, 36, http://dx.doi.org/10.15227/orgsyn.036.0036.

Jung, D.-H., Ko, Y.K., Jung, H.-T., 2004. Aggregation behavior of chemically attached poly(ethylene glycol) to single-walled carbon nanotubes (SWNTs) ropes. Mater. Sci. Eng. C 24, 117–121.

Khalil, K.M.S., Baird, T., Zaki, M.I., El-Samahy, A.A., Awad, A.M., 1998. Synthesis and characterization of catalytic titanias via hydrolysis of titanium(IV) isopropoxide. Colloid Surf. A 132, 31–44.

Klostergaard, H., 1958. Notes – esterification with trapping phase. J. Org. Chem. 23, 108–110.

Kozhevnikov, I., 1998. Catalysis by heteropoly acids and multicomponent olyoxometalates in liquid-phase reactions. Chem. Rev. 98, 171–198.

Kuwahara, Y., Kaburagi, W., Nemoto, K., Fujitani, T., 2014. Esterification of levulinic acid with ethanol over sulfated Si-doped ZrO_2 solid acid catalyst: study of the structure–activity relationships. Appl. Catal. A: Gen. 476, 186–196.

Le Bigot, Y., Delmas, M., Gorrichon, J.P., Gaset, A., 1982. Synthesis of furoates and furfurylic alcohol esters under very mild conditions using supported base catalysis. Synth. Commun. 12, 327–332.

Lee, C.K., Yu, J.S., Lee, H.J., 2002. Determination of aromaticity indices of thiophene and furan by nuclear magnetic resonance spectroscopic analysis of their phenyl esters. J. Heterocycl. Chem. 39–36, 12070–21217.

Leofantia, G., Padovan, M., Tozzola, G., Venturelli, B., 1998. Surface area and pore texture of catalysts. Catal. Today 41, 207–219.
Lichtenthaler, F.W., 2000. Ulmann's Encyclopedia of Industrial Chemistry. Wiley-VCH VerlagGmbh and Co. KGaA, Weinheim.
Lichtenthaler, F.W., Peters, S., 2004. Carbohydrates as green raw materials for the chemical industry. C. R. Chim. 7, 65–90.
Liu, Y., Lotero, E., Goodwin Jr., J.G., 2006. Effect of carbon chain length on esterification of carboxylic acids with methanol using acid catalysis. J. Catal. 243, 221–228.
López-Salinas, E., Hernández-Cortéz, J.G., Schifter, I., Torres-García, E., Navarrete, J., Gutiérrez-Carrillo, A., López, T., Lottici, P.P., Bersani, D., 2000. Thermal stability of 12-tungstophosphoric acid supported on zirconia. Appl. Catal. A: Gen. 193, 215–225.
Lucas, N., Kanna, N.R., Nagpure, A.S., Kokate, G., Chilukuri, S., 2014. Novel catalysts for valorization of biomass to value-added chemicals and fuels. J. Chem. Sci. 126, 403–413.
Madje, B., Patil, P., Shindalkar, S., Benjamin, S., Shingare, M., Dongare, M., 2004. Facile transesterification of β-ketoesters under solvent-free condition using borate zirconia solid acid catalyst. Catal. Commun. 5, 353–357.
Mandal, A., 1983. Indian J Chem. Sect. B: Org. Med. Chem. 22, 505.
Martínez, J., Nope, E., Rojas, H., Brijaldo, M., Passos, F., Romanelli, G., 2014. Reductive amination of furfural over Me/SiO_2-SO_3H (Me: Pt, Ir, Au) catalysts. J. Mol. Catal. A: Chem. 392, 235–240.
Martín-Muñoz, M.G., Fierros, M., Rodríguez-Franco, M.I., Conde, S., 1994. Mucor miehei lipase catalyzed transesterifications on aromatic and heteroaromatic substrates. A general survey. Tetrahedron 50, 6999–7008.
Massart, R., Contant, R., Fruchart, J., Ciabrini, J., Fournier, M., 1977. Phosphorus-31 NMR studies on molybdic and tungstic heteropolyanions. Correlation between structure and chemical shift. Inorg. Chem. 16, 2916–2921.
Mastikhin, V.M., Kulikov, S.M., Nosov, A.V., Kozhevnikov, I.V., Mudrakovsky, I.L., Timofeeva, M.N., 1990. ^{1}H and ^{31}P MAS NMR studies of solid heteropolyacids and $H_3PW_{12}O_{40}$ supported on SiO_2. J. Mol. Catal. A: Chem. 60, 65–70.
Osiglio, L., Romanelli, G., Blanco, M., 2010. Alcohol acetylation with acetic acid using borated zirconia as catalyst. Catal. A: Chem. 316, 52–58.
Patel, S., Purohit, N., Patel, A., 2003. Synthesis, characterization and catalytic activity of new solid acid catalysts, $H_3PW_{12}O_{40}$ supported on to hydrous zirconia. J. Mol. Catal. A: Chem. 192, 195–202.
Phonthammachai, N., Chairassameewong, T., Gulari, E., Jamieson, A.M., Wongkasemjit, S., 2003. Structural and rheological aspect of mesoporous nanocrystalline TiO_2 synthesized via sol–gel process. Micropor. Mesopor. Mater. 66, 261–271.
Pittelkow, M., Kamounah, F.S., Boas, U., Pedersen, B., Christensen, J.B., 2004. TFFH as an excellent reagent for acylation of alcohols thiols and dithiocarbamates. Synthesis 15, 2485–2492.
Pizzio, L.R., Blanco, M.N., 2003. Isoamyl acetate production catalyzed by $H_3PW_{12}O_{40}$ on their partially substituted Cs or K salts. Appl. Catal. A: Gen. 255, 265–277.
Polocci, P., Magnaghi, P., Angiolini, M., Asa, D., Avanzi, N., Badari, A., Bertrand, J., Casale, E., Cauteruccio, S., Cirla, A., Cozzi, L., Galvani, A., Jackson, P.K., Liu, Y., Magnuson, S., Malgesini, B., Nuvoloni, S., Orrenius, C., Sirtori, F.R., Riceputi, L., Rizzi, S., Trucchi, B., O'Brien, T., Isacchi, A., Donati, D., D'Alessio, R., 2013. Alkylsulfanyl-1,2,4-triazoles, a new class of allosteric valosine containing protein inhibitors. Synthesis and structure–activity relationships. J. Med. Chem. 56, 437–450.
Pope, M.T., 1983. Heteropoly Isopoly Oxometalates. Springer-Verlag, Heidelberg, pp. 180.
Qu, X., Guo, Y., Hu, Ch., 2007. Preparation and heterogeneous photocatalytic activity of mesoporous $H_3PW_{12}O_{40}/ZrO_2$ composites. J. Mol. Catal. A: Chem. 262, 128–135.
Raja, S., Xavier, N., Arulraj, S.J., 1989. Action of boron trifluoride etherate and stannic chloride on heterocyclic aromatic acetals. Indian J. Chem. Sect. B: Org. Chem. Med. Chem. 28, 687–689.
Rivera, T.S., Sosa, A., Romanelli, G.P., Blanco, M.N., Pizzio, L.R., 2012. Tungstophosphoric acid/zirconia composites prepared by the sol–gel method: an efficient and recyclable green catalyst for the one-pot synthesis of 14-aryl-14H-dibenzo [a, j] xanthenes. Appl. Catal. A: Gen. 443–444, 207–213.
Rob Van Veen, J.A., Veltmaat, F.T.G., Jonkers, G., 1985. A method for the quantitative determination of the basic, acidic, and total surface hydroxy content of TiO_2. J. Chem. Soc. Chem. Commun., 1656–1658.
Rocchiccioli-Deltcheff, C., Thouvenot, R., Franck, R., Spectres, I.R., 1976. díhétéropolyanions α-$MX_{12}O_{40}^{n-}$ de estructure de type keggin (X=B^{III}, Si^{IV}, Ge^{IV}, P^{V}, As^{V}, el M=W^{VI} et Mo^{VI}). Spectrochim. Acta 32A, 587–597.
Rubio, J., Otero, J.L., Villegas, M., Duran, P., 1997. Characterization and sintering behaviour of submicrometre titanium dioxide spherical particles obtained by gas-phase hydrolysis of titanium tetrabutoxide. J. Mater. Sci. 32, 643–652.
Serrano, J.C., Luque, R., Campelo, J.M., Romero, A.A., 2012. Continuous-flow processes in heterogeneously catalyzed transformations of biomass derivatives into fuels and chemicals. Challenges 3, 114–132.
Ke, S., Liu, F., Wang, N., Yang, Q., Qian, X., 2009. 1,3,4-Oxadiazoline derivatives as novel potential inhibitors targeting chitin biosynthesis: design, synthesis and biological evaluation. Bioorg. Med. Chem. Lett. 19 (2), 332–335.
Sheldon, R.A., 2000. Atom efficiency and catalysis in organic synthesis. Pure Appl. Chem. 72, 1233–1246.
Sing, W., Everett, D., Haul, R., Mouscou, L., Pierotti, R., Rouquerol, J., 1985. Reporting physisorption data for gas/solid system with special reference to the determination of surface area and porosity. Pure Appl. Chem. 57, 603–619.
Sosa, A., Rivera, T.S., Blanco, M.N., Pizzio, L.R., Romanelli, G.P., 2013. Tungstophosphoric acid supported on zirconia: a recyclable catalyst for the green synthesis on quinoxaline derivatives under solvent-free conditions. Phosphorus, Sulfur, Silicon Relat. Elem. 188, 1071–1079.
Tamura, M., Tonomura, T., Shimizu, K., Satsuma, A., 2012. CeO_2-catalysed one-pot selective synthesis of esters from nitriles and alcohols. Green Chem. 14, 984–991.
Thommes, M., Köhn, R., Fröba, M., 2002. Sorption and pore condensation behavior of pure fluids in mesoporous MCM-48 silica, MCM-41 silica, SBA-15 silica and controlled-pore glass at temperatures above and below the bulk triple point. Appl. Surf. Sci. 196, 239–249.
Won, J., Kim, H., Kim, J., Yim, H., Kim, M., Kang, S., Chung, H., Leeb, S., Yoona, Y., 2007a. Effective esterification of carboxylic acids using (6-oxo-6H-pyridazin-1-yl)phosphoric acid diethyl ester as novel coupling agents. Tetrahedron 63, 12720–12730.
Won, J.E., Kim, H.K., Kim, J.J., Yim, H.S., Kim, M.J., Kang, S.B., Chung, H.A., Lee, S.G., Yoon, Y.J., 2007b. Effective esterification of carboxylic acids using (6-oxo-6H-pyridazin-1-yl) phosphoric acid diethyl ester as novel coupling agents. Tetrahedron 63, 12720–12730.
Xu, X., Yang, Ch., Bu, D., Wang, H., Xu, J., 2013. Synthesis and insecticidal activities of cis-configuration nitenpyram analogues with benzoyl hydrazines. Heterocycl. Chem. 50, 945–948.
Yadav, G.D., Nair, J., 1999. Sulfate zirconia and it is modifies versions as promising catalysts for industrial processes. Rev. Micropor. Mesopor. Mater. 33, 1–48.
Yadav, G.D., Yadav, A.R., 2014. Synthesis of ethyl levulinate as fuel additives using heterogeneous solid superacidic catalysts: efficacy and kinetic modeling. Chem. Eng. J. 243, 556–563.
Zanetti, J.E., Beckmann, C.O., 1926. Esters of furoic acid. J. Am. Chem. Soc. 48, 1067–1069.
Zeitsch, K.J., 2000. The Chemistry and Technology of Furfural and its Many by-Products, 1st ed. Elsevier, Amsterdam, pp. 376.